Introduction

Motion at the nanoscale is one of the grand challenges of multidisciplinary nanotechnology while microfluidics are handled as the future of lab work due to the precise handling of low volumes, defined interfaces and scalability. Even though many applications can be tackled by combining these two research areas, just to name biosensors during the time of the fellowship we united both research areas for reaching two main goals: As synthetic approach and to obtain a defined interface for interfaces as swimming environment.

The report is split into two separate parts:

i) Synthetic endeavours in collaboration with Nicolas Hauck and Julian Thiele, IPF Dresden

State of the art

Up to now most micromotors are made out of hard, inorganic materials, causing problems like none tunable Young modulus, sharp and cutting edges, a lack of biodegradability and high material prices. Only few groups produced hydrogel-based microswimmers,[1] even though they have the potential solve all those issues with one single material for future microswimmers: Hydrogels are hydrophilic networks of polymer chains with different origins (from natural agarose to synthetic copolymers). They offer the possibility to produce Janus particles, i.e. particles with 2 different faces, named after the Roman god Janus. Employing microfluidics even different geometries (spherical, as platelets, rods, ovals) can be achieved. This anisotropy can be used to cause propulsion by selectively encapsulating catalytic agents into one half of the particles. Anisotropic distribution of products enables the asymmetric creation of gradients, a requirement for phoretic motion at the microscale.

Materials and methods

Chip production:Here, the chips are manufactured by combining photo and soft lithography.A master template is first created by spin-coating a negative photoresist onto a 3 inch siliconwafer(SiegertWafer, Aachen, Germany), subsequently illuminated with a shadow mask in a mask aligner (MJB3, SüssMicroTec, Garching, Germany). The non-illuminated parts of the photoresistare removed and a polydimethylsiloxane (PDMS)base and crosslinker mixture (Sylgard 184 silicone)is combined at a ratio 10:1 (w/w) and polymerized at 65°C for 1 h. The PDMS replica is bond by oxygen plasma treatment to a thin glass slide. To provide a hydrophobicmicrochannel surface, a solution of (tridecafluoro-1,1,2,2-tetrahydrooctyl)trichlorosilane (1 v/v%) in a fluorinated oil Novec 7500 (IoLiTec GmbH, Heilbronn, Germany) is injected into the channels and subsequently evaporated.

Microfluidics experiments: All experiments were performed high-precision syringepumps (Harvard Apparatus Pump 11 Pico Plus Elite, Harvard Apparatus, Holliston, MA, USA) employing PE tubing gastight syringes. To monitor droplet formation, microflow cells are operated on aninverted bright-field microscope (Primovert, Carl Zeiss AG, Oberkochen, Germany), equipped with a 10x objective lense (air), and coupled to a high-speed digital camera (Miro eX4, Vision ResearchInc., Wayne, MS, USA).

Fluid selection: continuous phase was HFE 7500 containing a low percentage (0.5%) of home-made ABA surfactant. Dispersed phase: 20% acrylamic was mixed with 2wt% methylenebisacrylamidin water. 0,5% LAP and dye were added and the solutions were handled carefully, strictly protected from light. The flow rates were varied to achieve different shapes and morphologies and the curing occurred by irradiation with focussed UV light. The obtained microgels were washed several times and subsequently imaged in Bright-field and fluorescence microscopy imaging of droplets and microgels isperformed on an inverted microscope (DMi8, Leica, Wetzlar, Germany).

Results and discussions

After several iterations of optimizing the conditions for both, the continuous phase (specifically the surfactant concentration) and the dispersed phase we found that several things increase the polymerization drastically:

- higher content of photoinitializer
- higher monomer content
- higher content of surfactant since it facilitates the migration of the photoinitializer into the oil phase
- smaller droplet sizes

After optimizing the conditions (UV, flow rates, phase ratio) particles were obtained (Fig. 1, b). Flowing two continuous phases in parallel resulted in hardly any mixing and due to the fast crosslinking process this strict separation could be maintained in the flow, the separate droplets after the junction and even in the microgel particles after curing. We found, that the particle morphology adapted to the channel geometry due to the fast polymerization process, which enabled us to adapt the particle geometry from round spheres to flat discs.

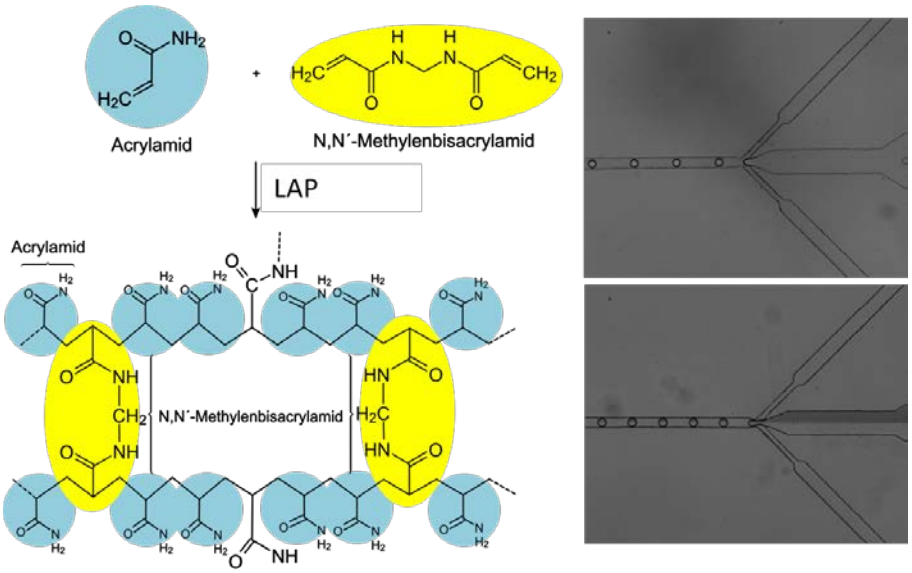

Fig. 1: Chemical composition of the selected system: the polymer is acrylamid, with methylenbisacrylamid as crosslinker and Lithium phenyl-2,4,6-trimethylbenzoylphosphinate as initializer.

The two different continuous phases were fluorescently labelled in order to enable fluorescent imaging (shown in fig. 2). After having obtained particles with Janus geometries we added 1wt.% of catalase to one of the dispersed phases in order

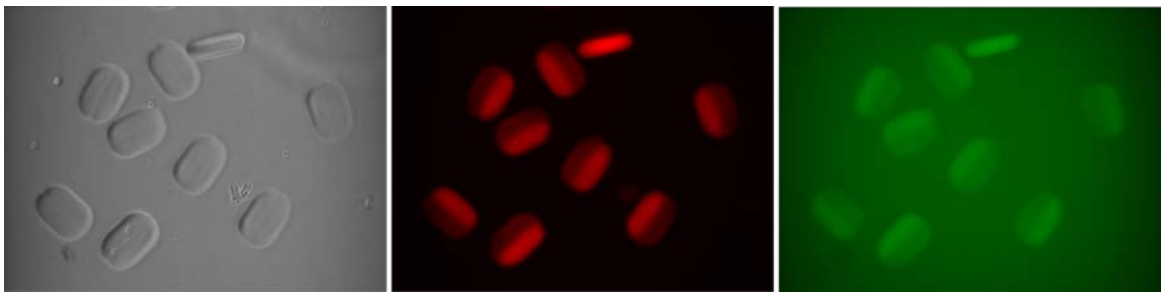

Fig. 2: Optical and fluorescence images of hydrogel particles. From left to right: bright field, Alexa vs Fluorescein channelshowing that both phases are polymerized without significant mixing.

to obtain active motion. However, the enzyme entrapment conditions are not yet optimized, some trials showed that catalase could be incorporated into the particles, however, ballistic swimming has not yet been achieved. One reason might be the photodamage of the enzyme. Beforehand we analysed the activity of catalase with a UV lamp at 365 nm without observing a significant decrease in activity, but the presence of a photoactivator and the focussing of the light within the microfluidic experiments might still have an unfavourable effect on the enzyme stability.

Conclusions

We successfully established and fine-tuned a microfluidic setup to create Janus particles based on Hydrogels. The manifold influences on the crosslinking step coming from polymer as well as crosslinker concentration, but also flow rates due to the changes in exposure time allow tuning a number of variables in the particles, such as morphology, chemical composition and therefore responsive- or stiffness and aspect ratio. The encapsulation of dyes allowed us the monitoring of the particle formation which happens without a larger influence of microscale mixing, resulting in well separated halves (see fig. 2). The catalytic content of the Janus particles was attempted by introducing catalase into the system, which still did not result in active propulsion despite the fact that bubble formation was observed. The reason for this delocalization of the bubbles needs to be investigated, which will be done by a measurement of the catalytic catalase activity after exposure to focussed UV light and contemporarily by the replacement of the catalase by catalytic Platinum nanoparticles.

ii) Microfluidic droplets as defined interfaces for microswimmers

State of the art

Nano- and micromotors perform selected mechanical movements and they are proposed for various applications ranging from drug delivery to waste water cleaning or sensor development. However, in most of these engineered environments the conditions are not static but dominated by different flows and interfaces. Therefore, significant efforts have been dedicated to study artificial micromotors in close proximity to solid walls.Creation of stable fluid-fluid interfaces is not a trivial task. The experimental studies of active matter on interfaces has mostly been performed in specially engineered cases, for example we studied the particle behavior close to a wedge formed by a droplet and a solid surface. Dietrich *et. al* studied the swimming of active Janus particles distributed at the liquid-liquid interface by spreading out an isopropanol solution directly at the boundary.[2] They found different wetting behavior for both particle phases, and they correlated the orientations of the particles with the two populations of particle speed they had observed. The group of Stocco studied the enhanced motion of particles on the water surface, as well as the wetting of Janus particles that had been sprayed at the water interface.[3,4] Spraying/spreading particles at the interfaces, leads to 'trapped particles' which are not able to release themselves from the interface or to move away from the boundary. Theoretical studies have considered particles that were free to attach to or leave the interface, but they were limited to fully active particles without considering the asymmetry that is present in Janus particles.[5,6]In collaboration with the group of P. Garstecki we developed a microfluidic system to study the active motion of platinum-capped microparticles at the liquid-liquid interface at different concentrations of surfactant in one of the phases. This combines a hydrodynamic trap with the evaluation of particles motion that are present at the liquid-liquid interface entirely in one of the phases, and are not trapped at the interface between the liquid phases.

Materials and methods

fabrication of the devices: We used the negative, specially designedPDMS molds to cast PDMS positive chips which were bonded to 0.14 mm-thick glass slides by treating them with plasma generated at a plasma cleaner (Harrick Plasma, USA), and subsequently placing them together. We rendered the surface of channels hydrophobic by filling the channels with Novec 1720 (3M, USA), and after evaporation at room temperature, we baked the chip at 75°C for one hour.
choice of fluids:For the continuous phase, we used Novec HFE 7500 (3M, USA) with PFPE-PEG-PFPE fluorosurfactant that was synthesized according to a previously described protocol.[7] For the experiments with varying the concentration of surfactant, we used Novec HFE 7500 with the addition of flurosurfactant at a concentration of 0.0025 % (w/w) for generation of droplets and merging of droplets in the *2D trap*, and Novec HFE 7500 with the addition of flurosurfactant at a concentration of 2.0 % (w/w) for changing the conditions at the interface of liquids. The dispersed phase was i) water with added microparticles, and ii) water with the addition of hydrogen peroxide at 3.0 % (w/w). The motion of fluids was generated and controlled with Nemesys syringe pumps (Cetoni, Germany) equipped with glass syringes (Hamilton, USA).
preparation of the particles: Janus particles were obtained by drop casting of a suspension of spherical silica colloids (2 and 5 µm diameter, Sigma-Aldrich) on an oxygen-plasma-cleaned glass slide followed by slow evaporation of the solvent. In an electron beam system high vacuum was applied and subsequently a monolayer of 2 nm Ti was evaporated to guarantee good adhesion of the 10 nm Pt for catalytic properties. To release particles from the glass slides into de-ionized (DI) water, short ultrasound pulses were sufficient.
imaging and detection: The locked droplet and the particles inside the droplet were recorded with an inverted confocal microscope Nikon A1 (Nikon, Japan), in bright field illumination. The recordings are generated at a frame rate of 12.5 frames per second. The videos were analyzed with a tracking software and the speed was obtained as an average of minimum 30 particles. The error bars are standard deviations.

Results and discussions

To study the motion of active particles we had to merge a droplet of hydrogen peroxide with a droplet containing microparticles, and we conducted the merging in the *2D trap.* Droplets of particles and droplets of hydrogen peroxide were generated at T-junctions, starting with a droplet of particles which was sent to the outlet 1 through the full barrier in the trap. This resulted in a metered droplet with particles locked inside the trap. Then, a droplet of hydrogen peroxide was generated in a T-junction, and was sent to the outlet 1 through the full barrier. The locked droplet of particles coalesced with the droplet of hydrogen peroxide due to compression merging[8] at a flow rate of 5 ml/h. The excess volume of the dispersed phase that was not locked in the trap, headed towards outlet 1. During all the recordings we describe here, there was no flow of liquids generated in the device. Outlet 2 was used when the evacuation of the droplet from the trap after an experiment was necessary: a droplet was generated at T-junction to merge with the trapped droplet, and the large combined droplet left the trap through the barrier with a slit towards outlet 2

To demonstrate the presence of the flat surface inside the locked droplet, we have performed pre-experiments with inert silica particles (Fig. 2). Particles sedimented at the bottom-most side of the droplet, and at a high concentration of particles a large portion of the particles resided at a similar radius of the discus-shaped droplets, probably indicating where the curvature of the droplet increases, and thus where the gutters of continuous phase are located. The diameter of the droplet is defined by the diameter of the trap and equals 1 mm. The diameter of the circle formed by the densely packed particles is 0.75 mm.

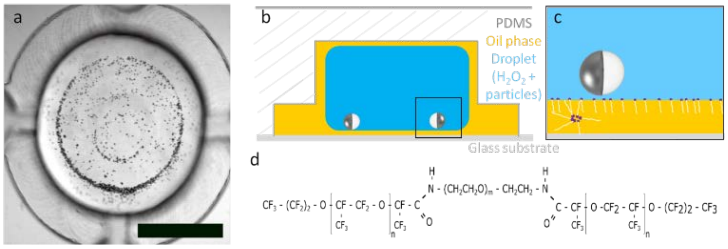

Fig. 1 a) Microparticles sediment in a circular pattern, revealing the location at which the discus-shaped droplet ceases to be flat. The particles gather at a similar radius around the center of the trap. Scale bar is 500 µm. b) Scheme of the system and c) Cartoon of a Janus particle at the liquid-liquid interface. d) Formula of the surfactant as described

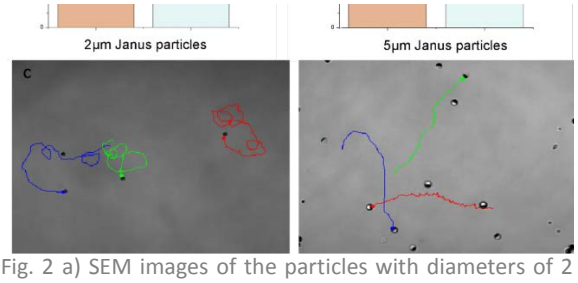

Fig. 2 a) SEM images of the particles with diameters of 2 µm (left) and 5 µm (right); b) speed distributions with standard deviations for small (left) and large (right) Janus particles on liquid-liquid interfaces (orange) compared with speeds at a solid glass substrate (light blue); c) sample trajectories of particles swimming on the oil interface with the particles displayed at the end of the track, the swimming proceeds towards the SiO_2 hemisphere (which appears white in the micrographs).

When a second droplet of 3% hydrogen peroxide with the same volume is merged in the trap, about half of the particles are flushed out of the trap, while the rest of the particles remain in the trap, forming a mixed phase of water/particle suspension and diluted peroxide. The peroxide that remains in the trapped droplet acts as fuel for the Janus particles. Immediately after merging the droplets the particle activity can be observed by a change in orientation of the particles. Just as we have observed on solid interfaces the orientation of the directional vector of the particles is of about 0° to the bottom flat interface (Fig. 1c).[9] The interface of liquids is covered with fluorosurfactant.The motion of the Janus colloids resembles strongly the motion on solid substrates in both morphology and speed values (Fig. 3). Since the particles are not able to settle directly at the interface, they rather approach it and act similarly as if they placed next to a solid wall, without showing indications of slipping effects at the boundary. A plausible interpretation might be the fixation of the interface by the surfactant as observed by Manor et al. in AFM measurements of the hydrodynamic forces at fluid-fluid boundaries.[10,11] These indicate a no-slip boundary condition that applies to oil/water interfaces in presence of surfactants and manifests in a tangentially immobile interface, even though the concentration of surfactant was maintained low to enable on-chip merging and coalescence of the two droplets.[12] Despite the fact that we cannot completely exclude any deformation of the surface by the particles, there is no visible indication that the active particles exert this kind of effect on the droplet . If the deformation were present it would probably be only of a subnanometer size order and would not be visible in an optical microscope.

The evaluation of the particle speeds shows that the speeds have relatively large speed distributions on both, glass and oil interfaces. Eventually, particles get trapped at the surface for some time, which is generally ascribed to surface inhomogeneities, e.g. roughness of the metal or not perfect coverage. Similar behavior is found also within the oil droplet, which can be confirmed by similar observations we made earlier on less defined oil surfaces (unpublished data). For the 2 µm particles a clear drop of speed is observed on the oil surface (Fig. 2b, left), which could be due to the fact that the HFE oil is able to absorb oxygen. However, the speed found for larger particles is not significantly changed compared to glass substrates (Fig. 2b, right). Even at very low concentrations the surfactant seems to lock the surface slip – which leads to a particle behavior similar to swimming on a solid interface. Only the speed for small particles is slightly decreased while larger particles show comparable speeds as on a reference glass surface. However, the behavior and speed of particles on solid surfaces are known to depend strongly on local conditions. The reduction of the speed of the particles can be due to the fact that HFE7500 absorbs gases (O_2) and is therefore able to decrease the product gradient.

Conclusions

Here we have found a trap design that allows metering droplets, merging droplets and changing the concentration of the surfactant in the oil while trapping the droplet. When merging two liquid phases that contain peroxide and active Janus particles, respectively, an activation of the Janus particles upon fuel addition is observed. The large flat surface is suitable

to follow the particle motion over microscopic distances. This elegant setup allows to study the motion of particles close to liquid-liquid surfaces without particles being trapped directly at the surface. The observed behavior in many features resembles the behavior at of particles at solid substrates, but allows the evaluation of different slip conditions. Since the use of active matter out of sterile and static lab environments will bring interfaces into play, the behavior after encountering these should be well understood.

References

1 A. Chen, X. Ge, J. Chen, L. Zhang and J.-H. Xu, *Lab Chip*, , DOI:10.1039/C7LC00950J.

2 K. Dietrich, D. Renggli, M. Zanini, G. Volpe, I. Buttinoni and L. Isa, *New J. Phys.*, , DOI:10.1088/1367-2630/aa7126.

3 X. Wang, M. In, C. Blanc, M. Nobili and A. Stocco, *Soft Matter*, 2015, **11**, 7376–7384.

4 X. Wang, M. In, C. Blanc, P. Malgaretti, M. Nobili and A. Stocco, *Faraday Discuss.*, 2016, **191**, 305–324.

5 P. Malgaretti, M. N. Popescu and S. Dietrich, *Soft Matter*, 2016, **12**, 4007–4023.

6 P. Malgaretti, M. N. Popescu and S. Dietrich, *Soft Matter*, , DOI:10.1039/C7SM02347B.

7 C. Holtze, A. C. Rowat, J. J. Agresti, J. B. Hutchison, F. E. Angile, C. H. J. Schmitz, S. Koster, H. Duan, K. J. Humphry, R. A. Scanga, J. S. Johnson, D. Pisignano, D. a Weitz, F. E. Angilè, C. H. J. Schmitz, S. Köster, H. Duan, K. J. Humphry, R. A. Scanga, J. S. Johnson, D. Pisignano and D. A. Weitz, *Lab Chip*, 2008, **8**, 1632–1639.

8 X. Niu, S. Gulati, J. B. Edel and A. J. deMello, *Lab Chip*, 2008, **8**, 1837–1841.

9 J. Simmchen, J. Katuri, W. E. W. E. Uspal, M. N. M. N. M. N. Popescu, M. Tasinkevych, S. Sánchez, S. S?nchez and S. Sánchez, *Nat. Commun.*, 2016, **7**, 10598.

10 O. Manor, T. T. Chau, G. W. Stevens, D. Y. C. Chan, F. Grieser and R. R. Dagastine, , DOI:10.1021/la204272u.

11 F. G. Ofer Manor, Ivan U. Vakarelski,| Geoffrey W. Stevens and and D. Y. C. C. Raymond R. Dagastine, *Langmuir*, 2008, **110**, 11533–11543.

12 J.-C. Baret, *Lab Chip*, 2012, **12**, 422–433.